Solar electricity supply isolines of generation capacity and storage

Wolf Grossmann[a,b], Iris Grossmann[c,1], and Karl W. Steininger[a,d]

[a]Wegener Center for Climate and Global Change, University of Graz, A-8010 Graz, Austria; [b]International Center for Climate and Society, University of Hawaii at Manoa, Honolulu, HI 96822; [c]Climate and Energy Decision Making Center, Carnegie Mellon University, Pittsburgh, PA 15213; and [d]Department of Economics, University of Graz, A-8010 Graz, Austria

Edited by Stephen Polasky, University of Minnesota, St. Paul, MN, and approved February 10, 2015 (received for review September 5, 2013)

The recent sharp drop in the cost of photovoltaic (PV) electricity generation accompanied by globally rapidly increasing investment in PV plants calls for new planning and management tools for large-scale distributed solar networks. Of major importance are methods to overcome intermittency of solar electricity, i.e., to provide dispatchable electricity at minimal costs. We find that pairs of electricity generation capacity *G* and storage *S* that give dispatchable electricity and are minimal with respect to *S* for a given *G* exhibit a smooth relationship of mutual substitutability between *G* and *S*. These isolines between *G* and *S* support the solving of several tasks, including the optimal sizing of generation capacity and storage, optimal siting of solar parks, optimal connections of solar parks across time zones for minimizing intermittency, and management of storage in situations of far below average insolation to provide dispatchable electricity. *G*–*S* isolines allow determining the cost-optimal pair (*G*,*S*) as a function of the cost ratio of *G* and *S*. *G*–*S* isolines provide a method for evaluating the effect of geographic spread and time zone coverage on costs of solar electricity.

large-scale solar network | photovoltaics | US super grid | solar intermittency | dispatchable solar electricity

Electricity from photovoltaics (PV) has achieved competitiveness in several regions and countries (1, 2). Due to rapidly decreasing manufacturing costs, the 2010s are predicted to be characterized by ongoing grid-parity events for 75–90% of the global electricity market (2–4). PV is the fastest-growing electricity technology. Between 1976 and 2013, global installed PV has grown by a factor of 2 every 2 y (5). With each doubling, costs have decreased by 20% (2, 6). Construction of large-scale solar installations has begun worldwide (1, 6–10); e.g., in 2013 developers in Spain applied for permits to construct 37.5 gigawatt peak. During peak periods, this would cover almost 10% of the EU27 load at costs of $0.07 to $0.08 per kilowatt hour.

The intermittent nature of solar energy appears to be the main remaining hindrance to widespread solar electricity generation. Intermittency can be mitigated or overcome through distributed solar networks (11–19). Establishing such networks is a natural next step if such networks can provide dispatchable electricity at low costs. Research groups and large industrial consortia have proposed several continental and transcontinental solar networks, including Desertec EUMENA (connecting Europe, North Africa, and the Middle East) (13, 16), an Asian–Australian energy infrastructure (14, 15), and the "US Solar Grand Plan" (12, 20), a predominantly renewable energy supply system using high-insolation areas in the US Southwest. These networks all still need large amounts of overcapacity and storage, even if solar, wind, and geothermal are combined (19, 21–24). A recent study designed to meet 1/5 of the US electricity demand from solar and wind includes overcapacity at up to 3 times the load (19, 21). Hence, methods are urgently needed that minimize costs through optimal site selection across time zones and through precise optimization of the necessary generation capacity *G* and storage *S*.

This paper discusses and uses the finding that the relationship between any feasible capacity *G* (sufficient to meet the load) and the corresponding minimum storage *S* required to meet a given load with this capacity has the form of smooth isolines that can be precisely calculated and mathematically approximated with analytic functions. This relationship holds for small and large individual sites and for networks of geographically distributed sites. A *G*–*S* isoline is the minimal curve along which a constant or variable load is met; it is the lower boundary of the feasible area of all *G* and *S* that allows meeting that load. It visualizes feasible minimum combinations of *G* and *S*, here referred to as "feasible pairs" (*G*,*S*). Fig 1 shows *G*–*S* isolines for one location and five network configurations (Table 1) for a constant load of 1MW. Here we use a constant load, as this facilitates comparison of sites and configurations, but isolines for a variable load with the same yearly consumption give very similar numbers and the same isoline relationship between *G* and *S* (*SI Materials and Methods* and Figs. S1 and S2). Along an isoline, increasing *S* decreases the required *G* by evening out daily and seasonal intermittency, while adding *G* reduces the required *S* by meeting the load directly also shortly after sunrise and before sunset (11, 19, 21).

Cost optimization involving (*G*,*S*) requires hourly insolation values at each site. Ideal is a consistent global data set of hourly insolation over at least 10 y at good spatial resolution (11, 24, 25). The NASA Solar Sizer data used here (26) come close by providing daily insolation for 20 y for a global grid of 1° × 1°, i.e., with cells of 1° × 1°. Each site used here is represented by one cell. The method proposed in ref. 11 processes these data into hourly values (*SI Materials and Methods* and Fig. S3).

While isolines between production factors are broadly used in microeconomics, it is not self-evident that solar insolation—which is

Significance

The recent sharp drop in the cost of photovoltaic (PV) electricity generation accompanied by globally rapidly increasing investment in PV plants calls for new planning and management tools for large-scale distributed solar networks. We found that pairs of electricity generation capacity *G* and storage *S*, such that *S* is minimal to provide a given dispatchable electricity capacity for a given *G*, exhibit a smooth relationship of mutual substitutability between *G* and *S*. These *G*–*S* isolines support the solution of several tasks. This includes optimizing the size of *G* and *S* for dispatchable electricity, optimizing connections between solar parks across time zones for minimizing intermittency, and management of storage in situations of far below average insolation.

Author contributions: W.G. designed research; W.G., I.G., and K.W.S. performed research; W.G. and I.G. analyzed data; and W.G., I.G., and K.W.S. wrote the paper.

The authors declare no conflict of interest.

This article is a PNAS Direct Submission.

Freely available online through the PNAS open access option.

[1]To whom correspondence should be addressed. Email: irisg@andrew.cmu.edu.

This article contains supporting information online at www.pnas.org/lookup/suppl/doi:10.1073/pnas.1316781112/-/DCSupplemental.

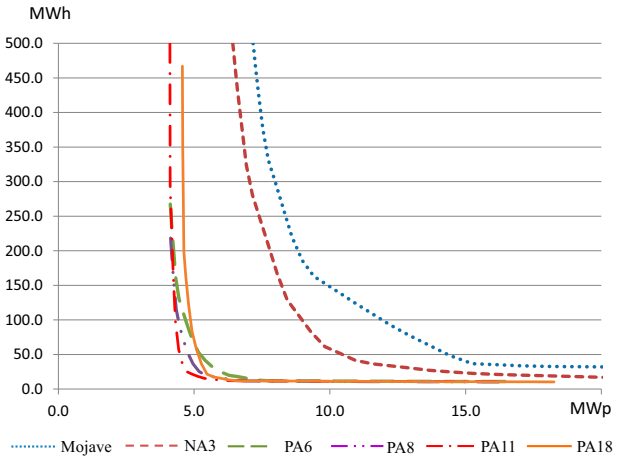

Fig. 1. *G–S* isolines for a site in the Mojave, the North American network NA3, and four Pan-American configurations (per 1 MW of load) (Table 1).

governed by attenuation and the overlap of the daily and seasonal cycles—will yield a smooth tradeoff between *G* and *S*. We found that this relationship holds for linear loads and for real hourly loads with considerable variation that fluctuate rapidly over time (*SI Materials and Methods*, Fig. S1, and the evaluation of that load in Fig. S2). The isoline relationship holds for hourly and daily insolation data in a 10 km × 10 km grid, for insolation from an isolated location with irradiation data at 10-min intervals and for arbitrary connections between up to 240 1° × 1° locations distributed over the whole globe, including Arctic and Antarctic locations with 6 mo of night (Fig. S4). Global networks can overlay different rhythms of day and night such that the network always has a high amount of radiation (Fig. S5). A combination of locations without night would be expected to hide or at least distort the hyperbolic shape of the respective isoline as the cosine pattern of daily solar radiation (27) is almost hidden under the overlay of manifold daily patterns. It is thus remarkable that *G–S* isolines for global networks still show the hyperbolic shape. Fig. 2 shows *G–S* isolines for PA6, a configuration connecting the three North American deserts with three South American deserts (Table 1). The 1-y isoline with variable load has higher demand for *G* and *S* than indicated by the 1-y isoline with constant load, and a lower one than indicated by the constant-load 20-y *G–S* isoline (*SI Materials and Methods*).

For all networks, we use uniform *G* across sites to simplify the analysis. Within-network optimization of *G* across a set of 100 globally distributed sites was at most 2.4% better than optimization with uniform *G* across these sites. The calculation of *G–S* isolines is described in *SI Materials and Methods*; empirically derived *G–S* isolines can be approximated with simple functions.

G–S isolines provide a simple, intuitive visualization of the suitability of different combinations of solar sites taking into account their geographic spread, time zone coverage, difference between summer and winter insolation, and attenuation. Fig. 1 shows *G–S* isolines for five distributed configurations of solar sites (Table 1) for a constant load of 1 MW. Isolines of productive high-insolation configurations are located in the lower left corner of the *G–S* coordinate system; less productive combinations are in the upper right. Hence, *G–S* isolines are an effective tool to support optimized site selection and to support the optimizing of electricity costs for both large-scale dispersed networks and small installations.

We discuss three applications of *G–S* isolines: first, the identification of maximum and minimum values of *G* and *S* across both the length of the time period and the size of the geographical area considered; second, tradeoffs between generation capacity or storage and transmission lines (configurations covering larger areas require lower values of *G* and *S* but need longer transmission lines); and third, storage power and combination and management of various storage types.

Results

Comparison of Solar Networks with *G–S* Isolines. Comparing the *G–S* isolines of several networks provides a visual illustration of how much each network is affected by intermittency, or, in other words, which networks need the least *G* and *S*. Fig. 1 compares the *G–S* isolines for a 1-MW load supplied by an isolated site in the Mojave, a network linking the three North American deserts (NA3) and four Pan-American networks that connect NA3 with the Atacama in Chile and adjacent deserts in Argentina and Bolivia (PA6, PA8, PA11, PA18, Table 1). Sites were selected based on high insolation and geographical spread. With the same *G* as the Pan-American networks, the Mojave site and NA3 need, respectively, the most and second-most *S* due to the lower insolation of the North American deserts and because the low geographic spread of NA3 offers only little compensation of intermittency. Connecting both hemispheres by linking NA3 with South American deserts in PA6 lowers the amount of *S* required. The least *S* is required for PA18. This is remarkable as PA18 includes the same six high-insolation deserts as PA6, PA8, and PA11 plus 12 lower-insolation sites. The reason for its lower storage requirements is that its larger geographic spread increases the number of sites that are unaffected by attenuation at a given time. Attenuation events on a 1- to 60-min timescale do not usually cover large areas due to the low correlation of such events across distances of 200 km or more (28).

Generally, *G–S* isolines are shifted to the right or upward (implying, respectively, higher *G* and *S*) for configurations covering fewer time zones, fewer degrees of latitude, or fewer sites. Connecting time zones decreases the effects of day and night; connecting both hemispheres compensates low winter insolation. *G–S* isolines give precise numbers for the substitution of *S* by *G* and vice versa. They also indicate the potential for substitution of *G* and *S* through transmission lines. The required *G* and *S* can be

Table 1. Sites of 1° × 1° included in the configurations in Fig. 1 and their basic characteristics

Name	Sites*	Sites	Maximum night hours, h	Maximum, minimum insolation, kWh·m^{-2}·d^{-1}
Mojave	Mojave desert	1	14	9.49,0.35
NA3	Three North American deserts: Mojave, Sonoran, Chihuahuan	3	14	9.05,1.05
PA6	NA3 and Atacama, Bolivia Litoral, Catamarca	6	9	7.3,3.1
PA8	PA6 and two tropical sites: Caatinga, Sechura I	8	8	7.15,3.41
PA11	PA8 and southern extension: Catamarca, Peru Interoceanica, Sechura II	11	8	7.31,3.94
PA18	PA11 and seven additional sites for extended geographic distribution (locations 1, 10, 18, 23, 33, 53, and 69 in Table S1)	18	7	6.51,2.35

Size of sites is 1° × 1° ~111.1 km × cosinus(radians(latitude)) × 40,000 km, i.e., at 0° 111.1 km × 111.1 km = 12,345 km^2, or at 36° 111.1 × 90 km = ~10,000 km^2.
*Details in *SI Materials and Methods* and Table S1.

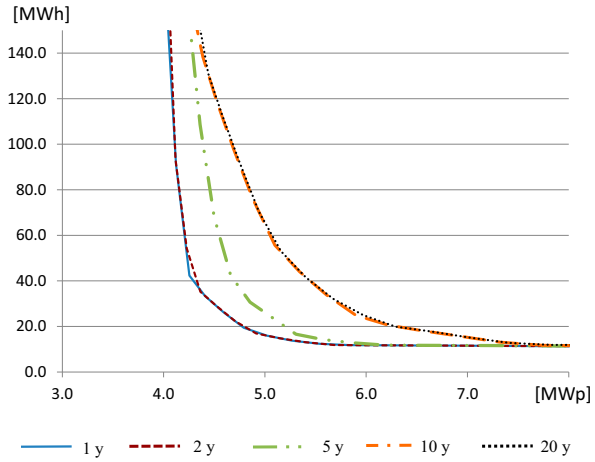

Fig. 2. *G–S* isolines for configuration PA6 (Table 1) for optimization over between 1 and 20 y and a 1-MW load. Years used: 1986, 1986–1987, 1986–1990, 1986–1995, and 1986–2005.

reduced through adding sites, yet this necessitates additional transmission lines, showing a tradeoff between costs of feasible pairs (*G*,*S*) and transmission costs. The least and most spatially extended configurations, NA3 and PA18, need, respectively, the lowest and highest total length of transmission lines but the highest and lowest amount of *S* for a given *G* and vice versa (Fig. 1). With the completion of the first very long distance high-voltage direct current (HVDC) lines of 1,000 miles or more in 2010 (29), further rapid cost decreases for HVDC lines are expected from the combined effects of learning and economy of scale (30), indicating the relevance of this tradeoff.

If transmission costs were forbidding, large networks would be impractical. With the advent of long-distance HVDC transmission (29, 30) and its practicality with the breakthrough of circuit breakers in 2013, transmission costs have decreased to such an extent that, for example, even a HVDC submarine cable between Europe and the United States has been calculated to be profitable for peak load (30). When comparing networks of increasing geographic extension, the minimal costs of their respective feasible pairs (*G*,*S*) show the maximal acceptable transmission costs for which the network would still be profitable.

To illustrate this, we calculate minimal electricity costs from an isoline with two different cost estimates for PV generation capacity *G* and battery storage *S*, $1,000/kWp (kilowatt peak) and $700/kWp for *G* and $250/kWh and $125/kWh for *S* (*SI Materials and Methods*: "high" and "intermediate" estimates). This gives the following two minimal cost estimates for dispatchable electricity without considering transmission: $207/MWh and $127/MWh for the Mojave, $171/MWh and $106/MWh for NA3, and $88/MWh and $55/MWh for PA6 (Table S2). Transmission costs increase sublinearly with line length (see *SI Materials and Methods*). With transmission costs of $3.50/MWh for NA3 and $24.50/MWh for PA6 (*SI Materials and Methods*), the resulting total electricity costs including transmission are $174.50/MWh and $109.50/MWh for NA3 and $112.50/MWh and $79.50/MWh for PA6. Even if transmission costs were several times higher, linking locations so that they form these networks gives electricity at lower costs than electricity from these locations if they are not linked. Using costs of dispatchable electricity from feasible pairs (*G*,*S*) allows an assessment of the maximum transmission costs such that networks would still be profitable. Thus, *G–S* isolines support a comparison of solar networks of different geographical spread to achieve optimal costs for dispatchable electricity.

Finding Cost-Optimal Feasible Pairs of (G,S). Generally, *G–S* isolines are shifted to the right or upward when more years of insolation are included, since this raises the probability of serious attenuation events. Fig. 2 shows *G–S* isolines from optimization time periods ranging from 1 y to 20 y for PA6 (the load is again 1 MW). The difference between the isolines from 5 y and 10 y of data are much higher than the difference between the isolines from 10 y or 20 y. The similarity of the isolines calculated from time periods of different lengths and their seeming convergence to an upper limit for all configurations considered here suggests that it may be possible to estimate *G–S* isolines with minimum *G* and *S* that are valid for very long time periods by increasing the values obtained from shorter time periods by some percentage. Future research should address this possibility.

G–S isolines can be used to evaluate storage options for lowering costs, both for large-scale distributed networks and for small installations. Fig. 3 illustrates this for the Pan-American configuration PA6 using a family of five *G–S* isolines that are derived, respectively, from 20 y of insolation data (1986–2005), 1 y of data (1986), 20 y with average insolation on each day, and composite years built from the least (most) solar insolation found for each specific day across the 20 y considered. We refer to the latter three as *G–S* isolines for average, minimum, and maximum insolation. The *G–S* isoline for average insolation is to the left of the isoline determined with the actual 20-y data, implying lower values of *G* and *S* (Fig. 3). This is because averaging reduces the influence of serious attenuation events. Hence, the corresponding values of *S* will not be sufficient for all cases. Maximal feasible pairs (*G*,*S*) are given by the *G–S* isoline for minimum insolation. Fig. 3 (*Top*) shows how the *G–S* isoline calculated from 20 y of actual insolation data are enclosed by the pessimistic *G–S* isoline for minimum insolation and the optimistic isolines obtained from average and maximum insolation. This bracketing of the *G–S* isoline obtained from 20 y of data with theoretical minimum and maximum isolines provides another way

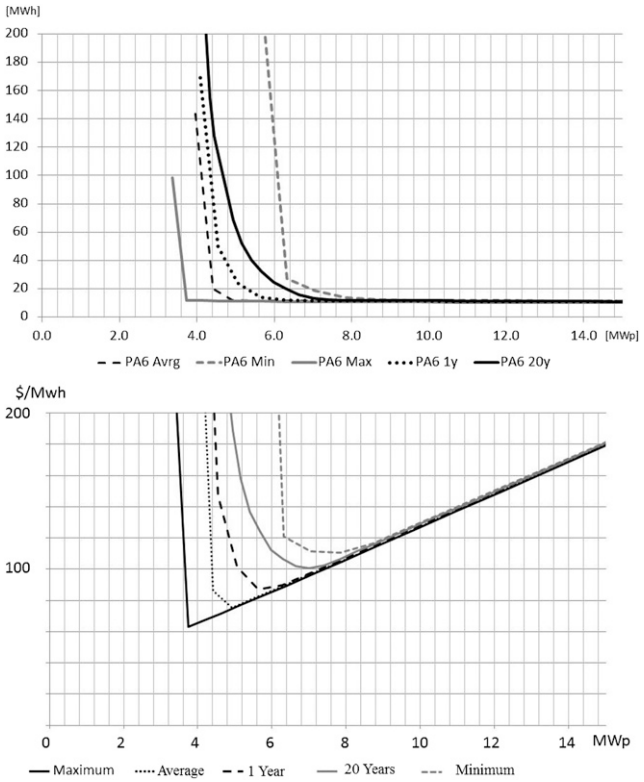

Fig. 3. (*Top*) *G–S* isolines for PA6 calculated respectively for 20 y (1986–2005), 1 y (1986), average insolation, minimum insolation, and maximum insolation. (*Bottom*) Electricity costs for the above *G–S* isolines.

to assess the trustworthiness of this isoline. Below, we apply this analysis to guide combination of different types of storage.

G–S isolines can be approximated with simple functions. Negative exponential functions are well suited for the asymptotic behavior of S for high values of G. The hyperbolic behavior of storage at low values of G requires a very large coefficient (4.08e7 in Eq. **1**); this approximation is only possible within a limited range of G and S. We tested hundreds of isolines; minimum costs of electricity were always in the range of G and S that can be approximated with an exponential function.

Let $(x,f(x))$ be a feasible pair with $f(x)$ the storage for generation capacity x and $g(x)$ the approximation to f(x). Then $(x,f(x))$ is approximated by $(x,g(x))$. For configuration PA6 with a 1-MW load we obtain (using kilowatts and kilowatt hours to avoid decimal places) (Fig. S6):

$$g(x) = 4.08e7 \exp(-0.0013x) + 11{,}000, \quad [1]$$

with an error for $x \in [5{,}000, 12{,}000]$ between −9.5% and 11.5%. Such functions allow constructing analytic equations that give the feasible pair $(x,g(x))$ for minimum costs of electricity. The cost c for 1 MWh electricity with $(x,g(x))$ using battery storage and excluding transmission costs is

$$c(x) = px + qg(x) + r; \quad c[\$], p[\$/MWp], x[MWp], q[\$/\text{MWh}], g[MWh], r[\$] \quad [2]$$

with p levelized cost of 1 MWp of G, q levelized cost of 1 MWh of S (31, 32), and r fixed costs per 1 MWh for this installation. This equation is valid for lithium ion battery storage used in solar installations. Li ion storage has many technological advantages and seems to become cost competitive (*SI Materials and Methods*). Li ion batteries have high round-trip efficiency of >90%. Typically, battery storage capacity S can be charged or discharged within at most 1 h (>1 S/h). Batteries handle interruptions in power well (31), for example in uninterruptible power supply packs. Other forms of storage need different versions of Eq. **2**. For example, compressed air energy storage (CAES) needs the term $qg(x)$ for its storage capacity and additional terms for its power concerning maximum charging and necessary output. One form of CAES consumes fuel, which would need an additional term in Eq. **2**.

With $dc(x)/dx = 0$ for minimization of $c(x)$ and using Eq. **1** for configuration PA6, the cost-optimal feasible x is

$$x = x\left(\frac{p}{q}\right) = -770 \ln\left(0.000019 \frac{p}{q}\right). \quad [3]$$

Fig. 3 (*Bottom*) shows electricity costs for the G–S isolines from Fig. 3 (*Top*) with costs of \$1,000/kWp for PV (\$800/kWp to \$1,500/kWp; see ref. 33 and *SI Materials and Methods*) and \$200/kWh for battery storage [(33) and *SI Materials and Methods*].

In the last 15 y, the cost p of generation capacity has decreased more rapidly than the cost q of storage. Given expected further changes of p/q, the calculation of the cost-optimal pair from the ratio p/q is of great interest. Fig. 4 compares the optimal feasible pair from the Solar Grand Plan (12, 20) with the optimal feasible pair found with the G–S isolines at 2012 costs. The latter requires less than 1/3 of the storage assumed by Zweibel et al. (12) at 28% higher generation capacity (21). Fig. 4 also shows that our calculation is compatible with the Solar Grand Plan (12, 20), as their optimal pair lies within the "secure" area given by the isoline (note that G and S in the Grand Plan are slightly higher than the extreme values given by our optimization). This figure also demonstrates an application of G–S isolines to the terawatt scale.

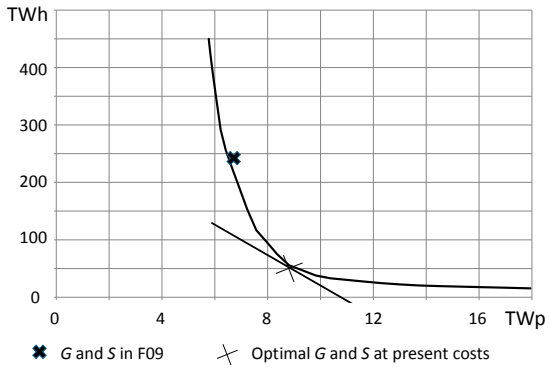

Fig. 4. G–S isoline for an NA3 configuration of the US Solar Grand Plan with ~3 TW of power (12, 20) with (G,S) as calculated by Fthenakis et al. (20) and cost optimization based on G–S isolines using present new values for costs of PV and storage.

In nondesert areas, the approximating functions can have higher maximum error as already 1 y of exceptionally bad weather can considerably deform the G–S isoline. In such cases, the cost-optimal feasible pair (G,S) can be found using the tangent of the G–S isoline with inclination p/q (Fig. 4).

The cost-optimal feasible pair can also be found numerically by multiplying G,S with their respective levelized annual costs, adding these two costs, and dividing the result by the integral over the load for 1 y. With the capital return factor CRF = 0.066 (6% interest rate, 40-y lifetime) and costs of \$700/kWp of installed PV, yearly PV costs are \$46.52/kWp per year. With CRF for batteries (6% interest rate, 20-y lifetime) = 0.087 and battery costs of \$125/kWh, yearly costs of batteries are \$10.90/kWh per year. With these costs for PV and batteries, the optimal feasible pair (7,549, 12,914) (Table S2) of PA6 for 1-MW load, i.e., 8,760 MWh per year, gives dispatchable electricity at (7,549 × \$46.52 + 12,914 × \$10.90)/8,760MWh = \$56.15/MWh. Optimal costs are found by comparing all cost numbers of an isoline; see Table S2 with data and costs for three G–S isolines from Fig. 1.

Effective Management Based on G–S Isolines. For high penetration with solar electricity a large number and variety of generation capacities, storage, transmission lines and power electronics will

Table 2. Characteristics of different storage types

Storage type	Costs capacity, \$/kWh	Costs power, \$/kW	Round-trip efficiency, %	Type of electricity	Long-term storage (>2 d)	Handles peak power
CAES	very low	Intermediate to high	50–70	AC	yes	no
Heat storage	low	intermediate	60–70	AC	no	no
Batteries	high	low	85–93	DC	yes	good
Supercapacitors	very high	low	95	DC	yes	excellent
Fly wheels	high	intermediate	70–90	AC	yes	fair
Super conducting	very high	low	98	DC	yes	excellent

All types are available; CAES, heat storage, and batteries are proven technologies.

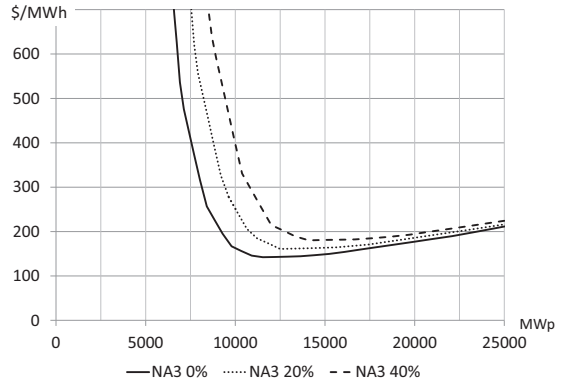

Fig. 5. *G–S* isolines for comparison of storage types with different round-trip efficiencies: ideal storage with 0% loss, storage with 20% loss, and storage with 40% loss (configuration NA3, per 1 MW of load).

be used. We will apply *G–S* isolines to support optimization combining different types of storage with different advantages and disadvantages (Table 2). Battery storage is expensive while offering important advantages including high round-trip efficiency > 90% and high power relative to the storage capacity *S* for both charging and discharging; typically, *S* can be discharged within 1 h ($\sim 1\ S/\text{h}$). Brief events of simultaneous low radiation in geographically well-distributed locations, as described in ref. 34, need high power. Batteries handle interruptions in power well (34), for example in uninterruptible power supply packs.

G–S isolines facilitate analyzing the issue of power for Li ion batteries with feasible pairs (*G,S*). The highest charging power among all networks considered in Table 1 comes from PA6, as the other networks additionally have locations with lower insolation. Each feasible pair (*G,S*) gives the highest charging power as a function of *G* and the capacity to accept this charge through its *S*. The cost-optimal feasible pair with the highest *G* is (7,409 kWp; 12,787 kWh) (*SI Materials and Methods* and Table S2). *G* = 7,409 kWp gives up to ~7,409 kW, as the solar constant is ~1 kW. The storage of 12,787 kWh in this feasible pair could accept 1 *S*/h, i.e., 12,787 kWh within 1 h, so it could even cope with PV up to 12,787 kWh. Scaling this to the available *G* gives 7,409/12,787 = 0.58 *S*. Meeting the load of 1,000 kW through discharging needs 1,000/12,787 *S*/h, i.e., ~0.08 *S*/h. Time series on actual load from European Network of Transmission System Operators for Electricity (ENTSO-E) show a variation in the load by factor 2.5 on an hourly scale. PA6 has the shortest nighttime, with ~9 h; meeting the load here might thus require ~2.5/9 *S*/h = 0.28 *S*/h. This is much less than the possible 1 *S*/h. Hence, with respect to power, even low-cost batteries may suffice.

In comparison with batteries, CAES can provide large energy storage at low costs [between $20/kWh (32) and $60/kWh (31)] if its compressed air is stored in underground caves that previously held natural gas (costs can vary significantly and are site specific). Rastler (31) reports that the incremental cost of an additional hour of storage once the cavern has been developed is $1/kW to $5/kW. CAES has a low round-trip efficiency of ~50% for storage times above 1–2 d, considerably increasing costs (Fig. 5). One may benefit from the low storage costs of CAES to the degree that CAES is charged only with excess electricity, does not use fuel, and is equipped with low power. Unless configurations are dispersed over a sufficient number of time zones, they experience nighttime. The power of storage of such configurations must be at least equal to the maximum load during nighttime.

For batteries, Eq. **2** takes these cost factors into account. We use configuration PA6 to describe a management scheme for dealing with unprecedented periods of long-term below-average insolation. Batteries are used as the main storage for this scheme, supported by CAES with very low power but large energy storage. Unprecedented periods of long-term low insolation put the dispatchability of a configuration at risk, even if calculated from a 20-y database. Maintaining adequate reserve capacity for rare uses can impose a substantial cost on the energy system, analogous to the high marginal cost associated with peak power production in existing systems.

Eq. **2** shows minimum electricity costs for about 7.3 MWp *G* for each 1-MW load over a 20-y time horizon. This holds for costs of *G* between $800/kWp and $1,500/kWp and costs of battery storage between $120/kWh and $350/kWh (including interest and depreciation; see *SI Materials and Methods*). As seen in Fig. 3 (*Top*), increasing *G* by 10% but keeping the values of *S* in all pairs (G, S) of the 20-y isoline gives a new *G–S* isoline with a very similar shape as the isoline for minimum insolation for values $G \geq 6$ MWp. As the isoline for minimum insolation would have given dispatchability even if all low-insolation events within the 20 y considered had occurred in 1 y, the 10% increase of *G* markedly enhances the protection against poor-insolation events of unprecedented severity. We add *G* in the form of CAES, as CAES provides electricity using its own generation capacity.

In PA6, the average insolation over 1 y is 2,233 kWh/m^2. This is 25.5% of a constant insolation of 1 kW/m^2 over the 8,760 h of 1 y, i.e., 25.5% is the capacity factor of PV in PA6, as the capacity factor gives the average actual energy from a given *G* over 1 y compared with the theoretical maximum energy that *G* could generate over 1 y. For solar, the actual insolation over 1 y (with day and night, seasons, and attenuation) is compared with a constant insolation of 1 kW/m^2, which represents the solar constant. With the capacity factor of CAES of ~90%, we calculate the required *G* (not *S*) in the form of CAES to give the same amount of electricity over 1 y as would be obtained with 10% more *G* in the form of PV as $10\% \times 0.25/0.90 = 2.7\%$; 2.7% more is an almost negligible amount of additional power. To verify that these predicted 2.7% are sufficient throughout the 20 y considered, we performed a sensitivity analysis with the most severe attenuation event within these 20 y when the storage of PA6 was fully depleted (the optimization allows momentary depletion of the storage as long as dispatchability is maintained throughout an event).

For the sensitivity analysis, we equip CAES with three sizes of power: 2%, 5%, and 10% of the load. CAES charges the batteries preemptively when their charge is below the maximum and weather forecasts predict insolation considerably below the long-term average. In Fig. 6, CAES is activated on December 12, 1986, when the main storage is below its maximum but still well charged, and switched off on December 30. Use of CAES to provide 2% additional power improves the minimum charge in the main storage from 0 to 4 MWh; 4 MWh could meet the load for 4 h on December 23, the most challenging day (Fig. 6). Fig. S7 shows details of charging and discharging for a similarly

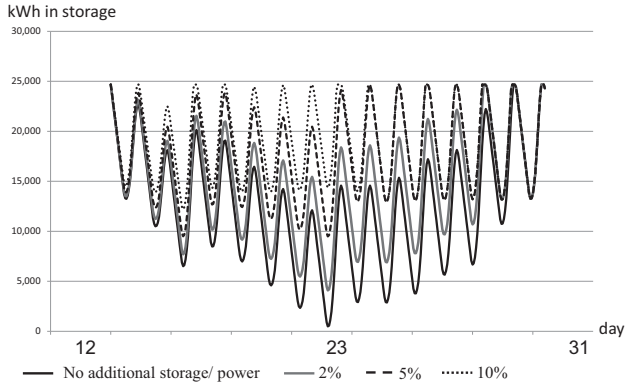

Fig. 6. Effective use of CAES at very low power for anticipatory management to cope with an event of extremely low insolation.

challenging day. Charging with 5% lifts the charge in the main storage to 9 MWh, which is the amount needed during the longest nighttime in PA6 (9.2 h); 10% additional power (Fig. 6) lifts the remaining charge on December 23 above the charge on a normal day (e.g., December 12), which is excessive. Thus, 2% of additional power is sufficient.

This example demonstrates how $G–S$ isolines can support testing different storage strategies for dealing with situations of extremely poor insolation. It also shows how $G–S$ isolines support research on combining different forms of storage. A more detailed analysis of the additional costs from using CAES is beyond the scope of this paper. The management scheme described above uses only CAES with very low power but for extended periods of time, thus decreasing depreciation costs. As CAES is charged only with excess electricity, no additional PV is needed. Otherwise, Fig. 5 would show the cost increase due to loss of electricity in storage. Costs from loss are minimized as batteries are the main storage and CAES uses only excess electricity. As excess electricity often costs money—typical costs at the Leipzig electricity stock market are, to date, $20/MWh—charging storage with excess electricity could increase profitability.

Discussion

$G–S$ isolines support planning and optimizing solar installations for dispatchable electricity. They facilitate site selection for large dispersed solar networks, support optimal choice among large configurations of solar sites, and allow optimization of G and S for both large-scale networks and smaller solar installations. Approximating functions as well as tangents to the $G–S$ isolines allow cost optimization under changing cost ratios of G and S. $G–S$ isolines, if evaluated with levelized costs of G and S, give cost curves for dispatchable electricity, based on which cost-optimal combinations of G and S can be determined. The storage management developed here extends the possibilities for cost optimization in situations of far below average insolation, analogous to the "merit order" approach that is used to bring generation capacity online in conventional electricity systems. $G–S$ isolines can be calculated in advance for operators of small solar installations, giving them a tool for assessment of possibilities and limitations of their configuration. $G–S$ isolines support planning, optimizing, and operating solar installations of different sizes, thus extending the potential of solar energy to become a major component of the global energy system.

Materials and Methods

A $G–S$ isoline is the curve combining minimal G and S along which a constant or variable load is met. To calculate the isolines, electricity from solar insolation at each location is added to the storage as long as capacity permits and the load is subtracted hourly as long as storage permits. The isolines have been calculated with a dynamic model and alternatively with a spreadsheet in which the storage is stepwise decreased such that the minimal charge becomes 0. An initial minimal value G_1 is calculated for a high amount of storage S_1 (e.g., for 20 y and a 1-MW load, $S_1 = 500$ MWh). The other points of the isoline are calculated by incrementally increasing G to up to 4 times its initial value, giving values G_2, G_3, ... and corresponding values of decreasing S_2, S_3, ... (see *SI Materials and Methods*).

ACKNOWLEDGMENTS. W.G. and K.W.S. were supported by research Grant 14451 of the Austrian National Bank (project DEVELOP), and I.G. and K.W.S. were supported by a research grant of the Climate and Energy Fund within the Austrian Climate Research Programme (project RE-ADJUST). I.G. was additionally supported by the Center for Climate and Energy Decision Making created through a cooperative agreement between the National Science Foundation (SES-0949710) and Carnegie Mellon University.

1. Dufo-Lopez R, Bernal-Agustin JL (2013) Photovoltaic grid parity in Spain. *Advances in Mechanical and Electronic Engineering, Springer Lecture Notes in Electrical Engineering Series*, eds Jin D, Lin S (Springer, Berlin, Heidelberg), Vol 178, pp 235–239.
2. Breyer C, Gerlach A (2013) Global overview on grid-parity. *Prog Photovolt Res Appl* 21:121–136.
3. Bazilian M, et al. (2012) *Re-Considering the Economics of Photovoltaic Power* (Bloomberg New Energy Finance, New York), WP 82.
4. Reichelstein S, Yorston M (2013) The prospects for cost competitive solar PV power. *Energy Policy* 55:117–127.
5. Maycock P (2013) *The Future of Energy Summit 2013* (Bloomberg New Energy Finance, New York). Available at bnef.com/Presentations/download/136. Accessed November 11, 2014.
6. Martínez-Duart JM, Hernández-Moro J (2013) Photovoltaics firmly moving to the terawatt scale. *J Nanophoton* 7(1):078599.
7. Schleicher-Tappeser R (2012) How renewables will change electricity markets in the next five years. *Energ Policy* 48:64–75.
8. Hand MM, et al., eds (2012) *Renewable Electricity Futures Study* (Natl Renewable Energy Lab, Golden, CO), NREL/TP-6A20-52409.
9. Li J (2009) Scaling up concentrating solar thermal technology in China. *Renew Sustain Energy Rev* 13:2051–2060.
10. Sims RE, et al. (2007) Energy supply. *Climate Change 2007: Mitigation. Contribution of Working Group III to the 4th Assessment Report of the Intergovernmental Panel on Climate Change 2007* (Cambridge Univ Press, Cambridge, UK).
11. Grossmann W, Grossmann I, Steininger K (2012) Distributed solar electricity generation across large geographic areas, Part I: A method to optimize site selection, electricity generation, and storage. *Renew Sustain Energy Rev* 25:831–843.
12. Zweibel K, Mason J, Fthenakis V (2008) A solar grand plan. *Sci Am* 298(1):64–73.
13. Viebahn P, Lechon Y, Trieb F (2011) The potential role of concentrated solar power (CSP) in Africa and Europe—A dynamic assessment of technology development, cost development and life cycle inventories until 2050. *Energ Policy* 39:4420–4430.
14. Taggart S, James G, Dong ZY, Russel C (2012) The future of renewables linked by a transnational Asian grid. *Proc IEEE* 100:348–359.
15. Blakers A, Luther J, Nadolny A (2012) Asia Pacific Super Grid —Solar electricity generation, storage and distribution. *Green* 2(4):189–202.
16. Trieb F, Schillings C, Pregger T, O'Sullivan M (2012) Solar electricity imports from the Middle East and North Africa to Europe. *Energ Policy* 42:341–353.
17. Meisen P, Pochert O (2006) *A Study of Very Large Solar Desert Systems with the Requirements and Benefits to Those Nations Having High Solar Irradiation Potential* (Global Energy Network Inst, San Diego).
18. Jacobson MZ, Delucchi MA (2011) Providing all global energy with wind, water and solar power, Part I: Technologies, energy resources, quantities and areas of infrastructure and materials. *Energ Policy* 39:1154–1169.
19. Budischak C, et al. (2013) Cost-minimized combinations of wind power, solar power and electro-chemical storage, powering the grid up to 99.9% of the time. *J Power Sources* 225:60–74.
20. Fthenakis V, Mason JE, Zweibel K (2009) The technical, geographical, and economic feasibility for solar energy to supply the energy needs of the US. *Energ Policy* 37:387–399.
21. Grossmann W, Grossmann I, Steininger K (2014) Distributed solar electricity generation across large geographic areas, Part II: A Pan-American energy system based on solar. *Renew Sustain Energy Rev* 32:983–993.
22. Heide D, Greiner M, von Bremen L, Hoffmann C (2011) Reduced storage and balancing needs in a fully renewable European power system with excess wind and solar power generation. *Renew Energy* 36:2515–2523.
23. Palmintier B, Hansen L, Levine J 2008), *Spatial and Temporal Interactions of Solar and Wind Resources in the Next Generation Utility* (SOLAR 2008, San Diego).
24. Brinkman G, Denholm P, Drury E, Margolis R, Mowers M (2011) Toward a solar powered grid. *IEEE Power Energy Mag* 9:24–32.
25. Tao C, Shanxu D, Changson C (2010) *Forecasting Power Output for Grid-Connected Photovoltaic Power System Without Using Solar Radiation Measurement* (Inst Electr Electron Eng, New York).
26. NASA (2010) *Radiation Budget Data Products: SSE Surface Meteorology and Solar Energy Data* (NASA Appl Sci Program, Greenbelt, MD).
27. Milone EF, Wilson W (2008) *Solar System Astrophysics: Background Science and the Inner Solar System* (Springer, New York).
28. Hummon M, Ibanez E, Brinkman G, Lew D (2012) *Sub-Hour Solar Data for Power System Modeling from Static Spatial Variability Analysis* (Natl Renewable Energy Lab, Golden, CO), NREL/CP-6A20-56204.
29. Åström U, Lescale VF, Menzies D, Weimin M, Zehong L (2010) The Xiangjiaba-Shanghai 800 kV UHVDC project, status and special aspects. *2010 International Conference on Power System Technology (POWERCON)* (Inst Electr Electron Eng, New York), pp 1–6.
30. Chatzivasileiadis S, Ernst D, Andersson G (2013) The global grid. *Renew Energy* 57: 372–383.
31. Rastler D (2010) *Electric Energy Storage Technology Options: A White Paper Primer on Applications, Costs, and Benefits* (Electr Power Res Inst, Palo Alto, CA), 1020676.
32. Mason J (2008) Coupling PV and CAES power plants to transform intermittent PV electricity into dispatchable electricity source. *Prog Photovolt Res Appl* 16(8): 649–668.
33. Osborne M (November 4, 2013) First Solar hits cost reduction milestone. *PVTech.* Available at www.pv-tech.org/news/has_first_solar_retaken_the_lowest_cost_pv_manufacturer_mantle.
34. Apt J, Fertig E, Katzenstein W (2012) Smart integration of variable and intermittent renewables. 45th Hawaii International Conference on System Science (HICSS) (Inst Electr Electron Eng, New York), pp 1997–2001.